photonics

MDPI

Communication

Development of a Mode-Locked Fiber Laser Utilizing a Niobium Diselenide Saturable Absorber

Weiqin Guo [1,2], Ling Zhang [2], Xiaosheng Xiao [3,*], Xingxing Li [1], Zhigang Yin [2,4], Hui Ning [1,2], Xin Zhang [1] and Xingwang Zhang [2,4]

[1] Joint Lab of Digital Optical Chip, Wuyi University, Jiangmen 529020, China; weiqinguo2023@163.com (W.G.); wyuxxli@163.com (X.L.); nh13073763152@163.com (H.N.); zhangxin800800@163.com (X.Z.)
[2] Key Lab of Semiconductor Materials Science, Institute of Semiconductors, Chinese Academy of Sciences, Beijing 100083, China; zhangling@semi.ac.cn (L.Z.); yzhg@semi.ac.cn (Z.Y.); xwzhang@semi.ac.cn (X.Z.)
[3] School of Electronic Engineering, Beijing University of Posts and Telecommunications, Beijing 100876, China
[4] Center of Materials Science and Optoelectronics Engineering, University of Chinese Academy of Sciences, Beijing 100049, China
* Correspondence: xsxiao@bupt.edu.cn

Abstract: The saturable absorber of niobium diselenide ($NbSe_2$), with a wide working bandwidth and excellent nonlinear optical response, was prepared using liquid-phase exfoliation. Its saturation intensity and modulation depth were 5.35 MW/cm^2 and 6.3%, respectively. Stable mode-locking with a center wavelength of 1558.7 nm of an erbium-doped fiber laser based on a $NbSe_2$ saturable absorber was successfully achieved. The maximum average output power of the mode-locked laser was 6.93 mW, with a pulse width of 1.3 ps and a repetition rate of 25.31 MHz at a pump power of 550 mW. The results show that $NbSe_2$ is a promising photoelectric modulation material owing to its excellent nonlinear optical properties.

Keywords: niobium diselenide; saturable absorber; nonlinear absorption characteristics; fiber laser; mode-locked laser

check for updates

Citation: Guo, W.; Zhang, L.; Xiao, X.; Li, X.; Yin, Z.; Ning, H.; Zhang, X.; Zhang, X. Development of a Mode-Locked Fiber Laser Utilizing a Niobium Diselenide Saturable Absorber. *Photonics* **2023**, *10*, 610. https://doi.org/10.3390/photonics10060610

Received: 27 April 2023
Revised: 19 May 2023
Accepted: 22 May 2023
Published: 25 May 2023

Copyright: © 2023 by the authors. Licensee MDPI, Basel, Switzerland. This article is an open access article distributed under the terms and conditions of the Creative Commons Attribution (CC BY) license (https://creativecommons.org/licenses/by/4.0/).

1. Introduction

Ultrashort pulse lasers have been widely applied in medical diagnosis, optical detection, material processing, precision machining and fiber communication due to their advantages of a narrow pulse width and high peak power [1–3]. Passive mode-locking technology is the main method used to achieve ultrashort pulse output. Compared with other lasers, fiber laser has the advantages of a low cost, compact structure, high efficiency, easy integration and good stability. Therefore, passive-mode-locked fiber lasers have become a research hotspot [4–6].

The passive mode-locked laser cannot be realized without the help of a saturable absorber (SA). Although the traditional semiconductor saturable absorption mirror (SESAM) has a mature preparation technology and high stability, it is expensive and has a narrow working band [7]. Therefore, it is necessary to explore new SAs. The detailed study of graphene material has aroused research interest in SAs based on two-dimensional (2D) materials. Researchers have found that many 2D materials exhibit special linear and nonlinear (e.g., saturable absorption) properties in terms of optics, ranging from visible to mid-infrared light. This research shows that 2D materials have many potential applications in optical devices [8–11]. Exploring 2D materials with excellent optical properties is a key factor in developing high-performance pulsed lasers [12].

To date, 2D materials with saturable absorption have been discovered, including graphene [13,14], black phosphorus (BP) [15,16], topological insulators (TIs) [17,18], MXenes [19,20] and transition metal dihalides (TMDs) [21–24]. Among them, TMDs have garnered considerable attention due to their fast saturation recovery time and large modulation depth [25–28]. TMDs have a chemical formula of MX_2, where M represents transition

metal elements (W, Mo, Nb, Ta) and X represents chalcogen elements (S, Se, Te) [29–32]. In recent years, $NbSe_2$ has become a hot research topic in TMDs due to its unique properties, such as an excellent photoelectric response, high carrier mobility and superconductivity [33–35], making it a popular candidate material for optoelectronic device applications. In 2018, Shi et al. deposited $NbSe_2$ quantum dots onto a D-type fiber to achieve mode-locked lasers that operate at 1 and 1.5 μm [36]. In 2020, Chen et al. prepared a $NbSe_2$ saturable absorber using the mechanical stripping method and realized a mode-locked pulse output with a central wavelength of 1036 nm and a pulse width of 174 ps [37]. In the same year, Yang obtained a mode-locked laser with a pulse width of 697 fs and a central wavelength of 1556.3 nm using an optical deposition method [38].

In this paper, we prepared an $NbSe_2$ SA using liquid-phase exfoliation (LPE). The nonlinear test results show that the saturation intensity, modulation depth and nonsaturable absorption were 5.35 MW/cm^2, 6.3% and 67.18%, respectively. We inserted the SA into an erbium-doped fiber laser, successfully achieving a stable mode-locked pulse laser output at pump powers ranging from 90 to 550 mW. At a pump power of 550 mW, the pulse width, repetition rate and average output power were 1.3 ps, 25.31 MHz and 6.93 mW, respectively. The center wavelength of the mode-locked laser was 1558.7 nm. The root mean square (RMS) instability of the mode-locked laser at the pump power of 550 mW was less than 1%. We achieved a higher output power and more stable laser output than other reported results of mode-locked lasers based on $NbSe_2$ SA. The experimental results show that $NbSe_2$ has excellent nonlinear optical properties and future applications in ultrafast photonics devices.

2. Preparation and Characterization

In our experiment, $NbSe_2$ nanosheets were prepared using the LPE method due to its low cost, simple operation and easy realization of large-scale preparation. Firstly, we added 50 mg of sodium dodecyl sulfate (SDS) and 300 mg of polyvinyl alcohol (PVA) to 20 mL of deionized water (DI), heated it to 90 °C, and kept it for half an hour to fully dissolve the SDS and PVA. Secondly, we added 100 mg of $NbSe_2$ powder to the above solution and placed it in an ultrasonic cleaning machine for 10 h. Finally, the mixed solution was centrifuged at a speed of 5000 rpm for 1 h, and $\frac{1}{2}$ of the supernatant was taken to make the $NbSe_2$ nanosheet solution used in our experiment. The nanosheet solution was dropped onto the fiber jumper and the fiber was dried in the drying cabinet for 24 h. As shown in Figure 1, we deposited $NbSe_2$-PVA on the end face of the fiber jumper.

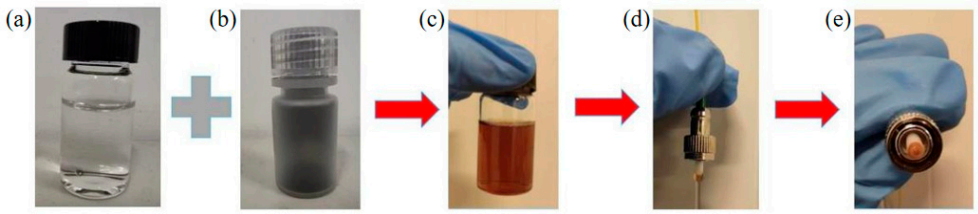


Figure 1. Preparation process of $NbSe_2$-PVA SA. (**a**) SDS and PVA mixture. (**b**) $NbSe_2$ powder. (**c**) $NbSe_2$-PVA dispersion. (**d**) Dispersion was dropped onto fiber end face. (**e**) $NbSe_2$-PVA was deposited on fiber end face.

The nanosheet solution was spin-coated onto the silicon substrate for characterization. Raman spectroscopy was used to characterize $NbSe_2$ nanosheets, and the corresponding results are presented in Figure 2. Figure 2a illustrates that two peaks were observed at 227.7 and 238.5 cm^{-1}, which correspond to the A_{1g} and $E^1{}_{2g}$ vibrational modes of $NbSe_2$, respectively. These findings are similar to those reported previously [38]. The scanning electron microscopy (SEM) image of the $NbSe_2$ nanosheets is shown in Figure 2b. $NbSe_2$ nanoparticles were uniformly distributed on the substrate. Furthermore, atomic force microscopy (AFM) was employed to characterize the material. As illustrated in Figure 2c, the thickness of $NbSe_2$ nanosheets was about 50 nm according to the marked line profiles.

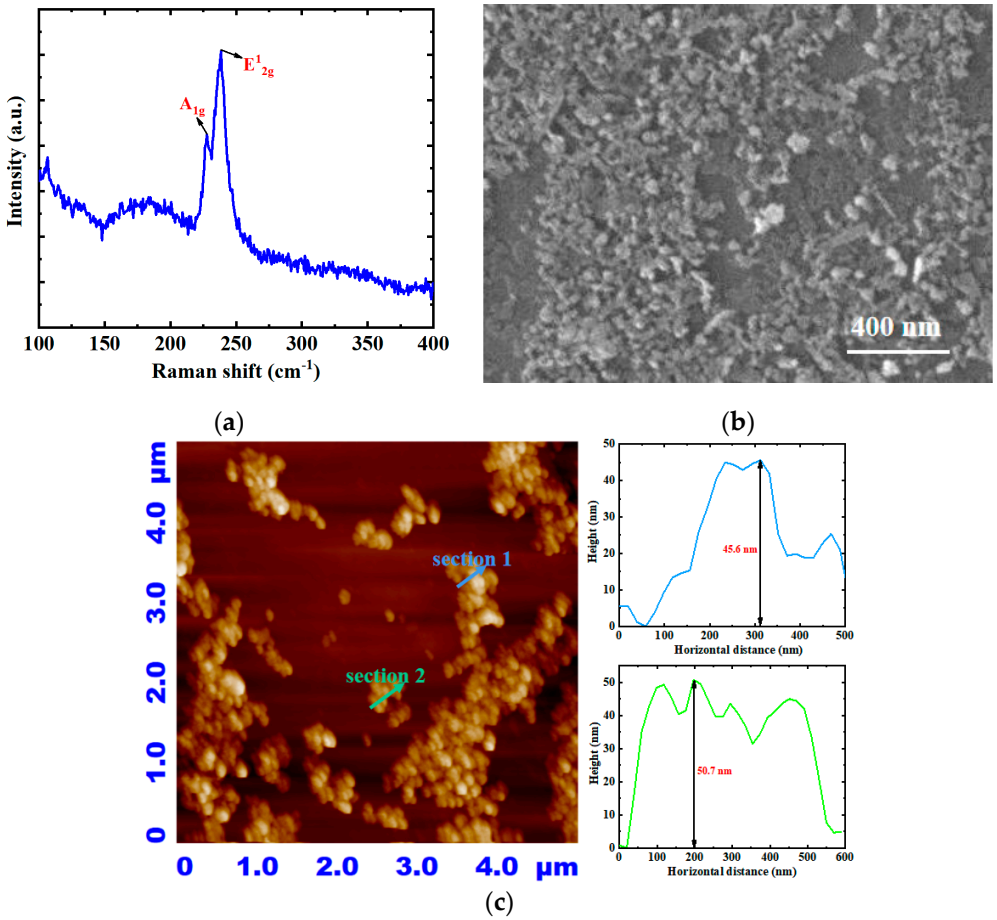
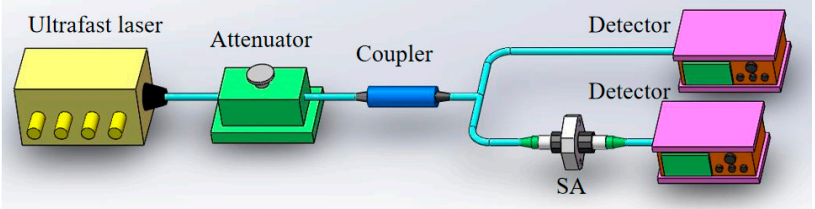


Figure 2. (**a**) Raman spectrum of $NbSe_2$ nanosheets. (**b**) SEM image of $NbSe_2$ nanosheets. (**c**) AFM image of $NbSe_2$ nanosheets.

A technique using a balanced twin-detector measurement was used to measure the saturable absorption characteristics of $NbSe_2$ nanosheets. The experimental setup is illustrated in Figure 3a. The pump laser, with a tunable wavelength in the near-infrared range, has a pulse duration of 300 fs and a repetition rate of 75 kHz. The experimental results were fitted using a non-linear transmission function. The relationship between light transmittance T and incident light intensity I can be described as follows [39]

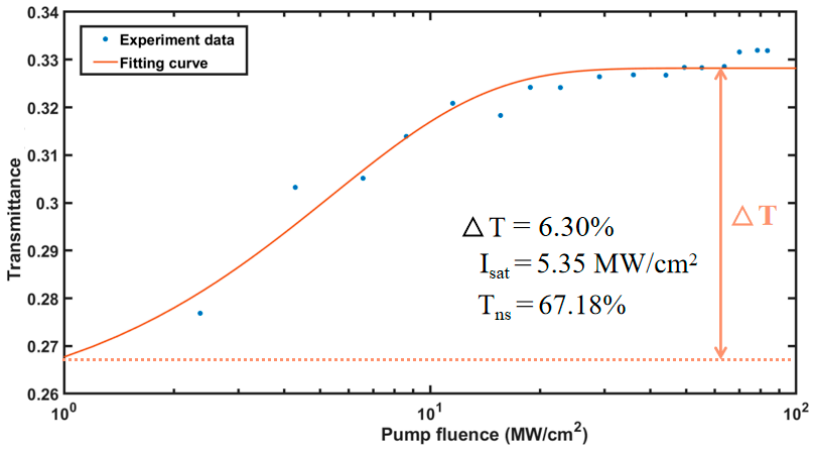
$$T = 1 - \frac{\triangle T}{1 + I/I_{sat}} - T_{\mathrm{ns}} \quad (1)$$

where ΔT is the modulation depth, I_{sat} is the saturation intensity, and T_{ns} is the nonsaturable absorption. The dependence of transmittance on the pump fluence is shown in Figure 3b. According to the fitting results, the modulation depth, saturation intensity and nonsaturable loss of $NbSe_2$ SA are determined to be 6.3%, 5.35 MW/cm^2 and 67.18%, respectively.



(**a**)

Figure 3. *Cont.*



(**b**)

Figure 3. (**a**) Balanced twin-detector measurement system. (**b**) Nonlinear transmittance diagram of $NbSe_2$ nanosheets.

3. Results and Discussion

The experimental setup of mode-locked fiber laser based on $NbSe_2$-PVA SA is depicted in Figure 4. A ring cavity structure was adopted, including a pump source (a 976 nm laser diode LD), 976/1550 nm wavelength division multiplexer (WDM), erbium-doped fiber (EDF), polarization controller (PC), polarization-independent isolator (PI-ISO), $NbSe_2$-PVA SA, single-mode fiber and 90/10 output coupler (OC). The pump light was coupled to the laser cavity through 976/1550 nm WDM. A 0.7 m single-mode erbium-doped fiber (Er80-8/125) was employed as the laser gain medium. PC was applied to adjust the polarization state of the laser. We used PI-ISO to ensure the unidirectional propagation of light in the laser cavity. The 90/10 OC was applied to the output laser. The total length of the ring laser cavity is about 8 m.

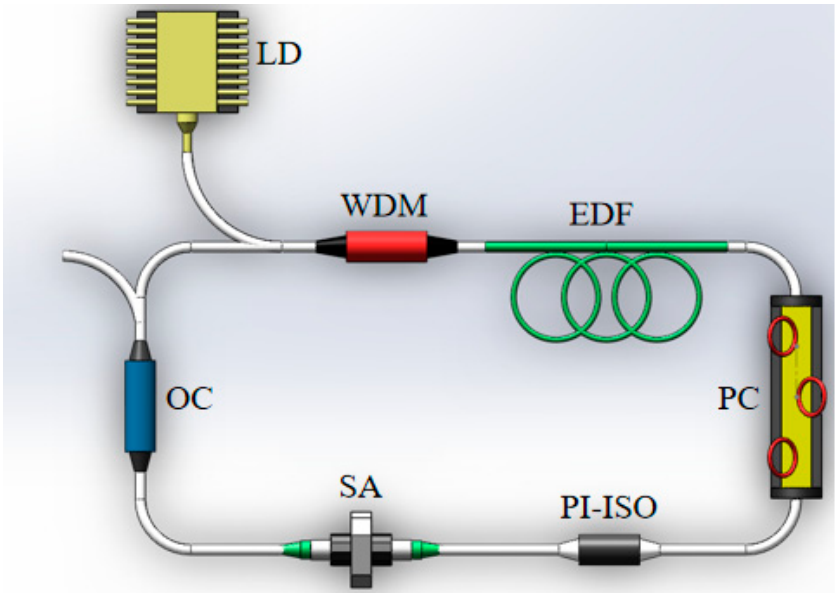


Figure 4. Erbium-doped mode-locked fiber laser based on $NbSe_2$-PVA SA.

During the mode-locked experiment, the PC was adjusted to change the polarization state in the cavity. The laser pulse was observed using 5 GHz photodiode (Thorlabs, DET08CFC/M) and 500 MHz real-time oscilloscope (KEYSIGHT DSOX3052T). At a pump power of 90 mW, the laser changed from continuous light to a mode-locked pulse, which

was observed using the real-time oscilloscope. A stable mode-locked laser was obtained as the pump power was further increased, from 90 to 550 mW.

At a pump power of 550 mW, the pulse sequence diagram of the mode-locked laser observed by the oscilloscope is illustrated in Figure 5a. The pulse interval is about 39.5 ns, corresponding to a repetition rate of 25.31 MHz, which is consistent with the result estimated from the cavity length. Then, the mode-locked laser spectrum was measured by a spectral analyzer (Agilent 86142B) with a resolution of 0.06 nm, and the result is demonstrated in Figure 5b. The center wavelength of the mode-locked pulse is 1558.7 nm, and the 3 dB bandwidth is 4.69 nm. The mode-locked laser was measured with an autocorrelator (A.P.E. pulseCheck), and the data are shown in Figure 5c by the sech^2 fitting. The full width at half maximum (FWHM) of the autocorrelation trace is 2 ps, which means that the pulse duration is 1.3 ps, assuming a hyperbolic secant shape. The calculated time-bandwidth product (TBP) is 0.753, whereas the theoretical limit value of TBP is 0.315. Our experimental results indicate that the mode-locked pulse has some chirp. Figure 5d shows the radio frequency (RF) spectrum measured by an RF signal analyzer (Agilent N9020 A). The repetition rate of the mode-locking laser is 25.31 MHz, and the signal-to-noise ratio (SNR) reaches 80 dB, indicating a highly stable mode-locking operation. Figure 5e demonstrates the relationship between the output power and pump power. At a pump power of 550 mW, the output power is 6.93 mW and the corresponding optical conversion efficiency is calculated to be 1.26%. The calculated single pulse energy and peak power are about 0.27 nJ and 207.7 W, respectively. To test the stability of the laser, the output power curve of the mode-locked laser for 30 min at a pump power of 550 mW was measured, as shown in Figure 5f. The calculated RMS instability of the output power of the mode-locked laser is less than 1%.

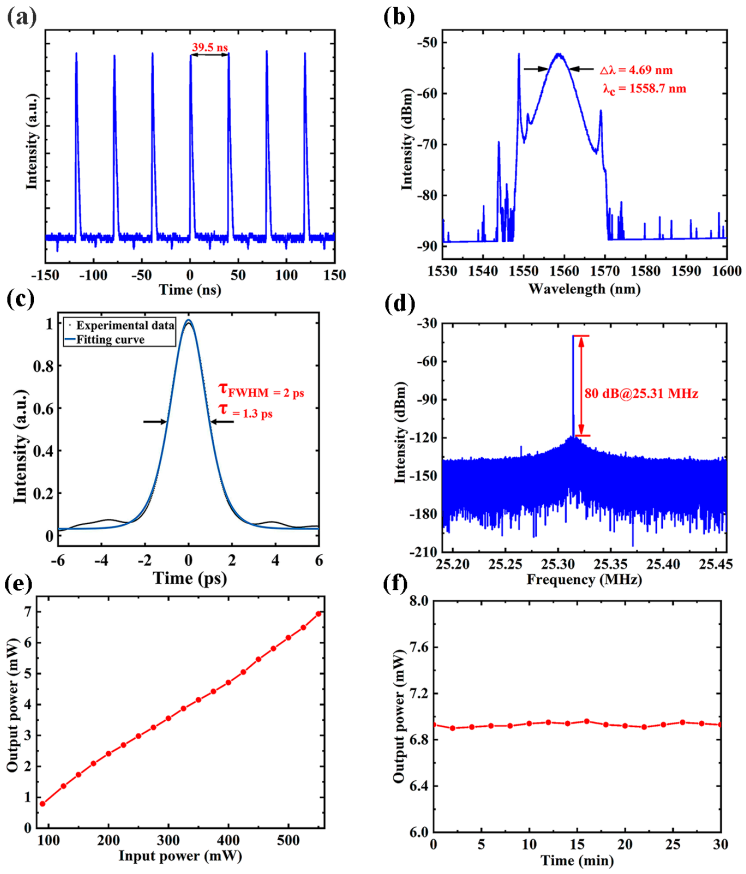


Figure 5. Output characteristics of the laser at 550 mW pump power. (**a**) Pulse train. (**b**) Spectrogram. (**c**) Autocorrelation trace. (**d**) RF spectrum. (**e**) Relationship diagram between the output power and pump power. (**f**) Stability of output power of mode-locked laser at pump power of 550 mW.

Removing the $NbSe_2$-PVA SA from the cavity and observing that no mode-locked pulsed laser is generated, even after adjusting the polarization controller and changing the pump power, confirms that the mode-locked operation is indeed caused by the $NbSe_2$-PVA SA.

4. Conclusions

In summary, we prepared an $NbSe_2$-PVA saturable absorber using LPE and inserted it into a homemade erbium-doped fiber laser. The laser produced stable mode-locked pulses with an output power of 6.93 mW, a center wavelength of 1558.7 nm, a repetition rate of 25.31 MHz, and a pulse width of 1.3 ps at a pump power of 550 mW. The output power of the mode-locked laser was measured for 30 min at the maximum pump power. The RMS instability of the output power was less than 1%. The results suggest that $NbSe_2$ has excellent nonlinear optical properties and promising applications in the field of ultrafast lasers.

Author Contributions: Conceptualization, X.X.; methodology, X.L.; investigation, W.G. and H.N.; resources, L.Z.; data curation, W.G. and L.Z.; writing—original draft preparation, W.G and X.Z. (Xin Zhang); writing—review and editing, W.G., L.Z. and X.X.; supervision, X.Z. (Xingwang Zhang) and Z.Y.; project administration, L.Z. and X.L. All authors have read and agreed to the published version of the manuscript.

Funding: This work is financially supported by Beijing Municipal Science & Technology Commission, Administrative Commission of Zhongguancun Science Park (No. Z211100004821006).

Institutional Review Board Statement: Not applicable.

Informed Consent Statement: Not applicable.

Data Availability Statement: The data of this study are available from the corresponding author upon reasonable request.

Acknowledgments: The authors would like to thank Chenxin Gao of Department of Precision Instruments, Tsinghua University for help on the characterization of the SA.

Conflicts of Interest: The authors declare no conflict of interest.

References

1. Ahmad, H.; Muhammad, F.D.; Pua, C.H.; Thambiratnam, K. Dual-Wavelength Fiber Lasers for the Optical Generation of Microwave and Terahertz Radiation. *IEEE J. Sel. Top. Quantum Electron.* **2014**, *20*, 166–173. [CrossRef]
2. Hu, P.; Mao, J.; Nie, H.; Wang, R.; Zhang, B.; Li, T.; He, J.; Yang, K. Highly Stable Passively Q-Switched Erbium-Doped All-Fiber Laser Based on Niobium Diselenide Saturable Absorber. *Molecules* **2021**, *26*, 4303. [CrossRef]
3. Zheng, J.-C.; Yang, S.; Zhu, Z.-W.; Lau, K.-Y.; Li, L. 72-fs Er-doped Mamyshev Oscillator. *J. Light. Technol.* **2021**, *40*, 2123–2127. [CrossRef]
4. Zhao, L.; Tang, D.; Wu, X.; Zhang, H.; Lu, C.; Tam, H.Y. Observation of dip-type sidebands in a soliton fiber laser. *Opt. Commun.* **2010**, *283*, 340–343. [CrossRef]
5. Yang, S.; Zhang, Q.-Y.; Zhu, Z.-W.; Qi, Y.-Y.; Yin, P.; Ge, Y.-Q.; Li, L.; Jin, L.; Zhang, L.; Zhang, H. Recent advances and challenges on dark solitons in fiber lasers. *Opt. Laser Technol.* **2022**, *152*, 108116. [CrossRef]
6. Yang, S.; Li, F.; Gong, M.-M.; Zhang, L.; Zhu, Z.-W.; Shen, H.-B.; Chen, S.-C. Generation of Q-switched and mode-locked pulses based on PbS/CdS saturable absorbers in an Er-doped fiber laser. *J. Mater. Chem. C* **2022**, *10*, 5956–5961. [CrossRef]
7. Gomes, L.; Orsila, L.; Jouhti, T.; Okhotnikov, O. Picosecond SESAM-Based Ytterbium Mode-Locked Fiber Lasers. *IEEE J. Sel. Top. Quantum Electron.* **2004**, *10*, 129–136. [CrossRef]
8. Novoselov, K.S.; Geim, A.K.; Morozov, S.V.; Jiang, D.; Katsnelson, M.I.; Grigorieva, I.V.; Dubonos, S.V.; Firsov, A.A. Two-dimensional gas of massless Dirac fermions in graphene. *Nature* **2005**, *438*, 197–200. [CrossRef]
9. Zhang, Y.B.; Tan, Y.W.; Stormer, H.L.; Kim, P.H. Experimental observation of the quantum Hall effect and Berry's phase in graphene. *Nature* **2005**, *438*, 201–204. [CrossRef]
10. Mak, K.F.; Lee, C.G.; Hone, J.; Shan, J.; Heinz, T.J. Atomically thin MoS_2: A new direct-gap semiconductor. *Phys. Rev. Lett.* **2010**, *105*, 136805. [CrossRef]
11. Qi, Y.; Yang, S.; Wang, J.; Li, L.; Bai, Z.; Wang, Y.; Lv, Z. Recent advance of emerging low-dimensional materials for vector soliton generation in fiber lasers. *Mater. Today Phys.* **2022**, *23*, 100622. [CrossRef]
12. Lu, S.; Wen, S.; Du, L.; Kang, Z.; Li, J.; Huang, B.; Jiang, G.; Miao, L.; Qin, G.; Zhao, C. Stable Dissipative Soliton Generation From Yb-Doped Fiber Laser Modulated via Evanescent Field Interaction With Gold Nanorods. *IEEE Photon. J.* **2018**, *10*, 1–8. [CrossRef]

13. Zhang, H.; Tang, D.; Knize, R.J.; Zhao, L.; Bao, Q.; Loh, K.P. Graphene mode locked, wavelength-tunable, dissipative soliton fiber laser. *Appl. Phys. Lett.* **2010**, *96*, 111112. [CrossRef]
14. Bonaccorso, F.; Sun, Z.; Hasan, T.; Ferrari, A.C. Graphene photonics and optoelectronics. *Nat. Photon* **2010**, *4*, 611–622. [CrossRef]
15. Xia, F.; Wang, H.; Jia, Y. Rediscovering black phosphorus as an anisotropic layered material for optoelectronics and electronics. *Nat. Commun.* **2014**, *5*, 4458. [CrossRef]
16. Sotor, J.; Sobon, G.; Kowalczyk, M.; Macherzynski, W.; Paletko, P.; Abramski, K.M. Ultrafast thulium-doped fiber laser mode locked with black phosphorus. *Opt. Lett.* **2015**, *40*, 3885–3888. [CrossRef]
17. Zhao, C.; Zou, Y.; Chen, Y.; Wang, Z.; Lu, S.; Zhang, H.; Wen, S.; Tang, D. Wavelength-tunable picosecond soliton fiber laser with Topological Insulator: Bi_2Se_3 as a mode locker. *Opt. Express* **2012**, *20*, 27888–27895. [CrossRef]
18. Liu, H.; Zheng, X.-W.; Liu, M.; Zhao, N.; Luo, A.-P.; Luo, Z.-C.; Xu, W.-C.; Zhang, H.; Zhao, C.-J.; Wen, S.-C. Femtosecond pulse generation from a topological insulator mode-locked fiber laser. *Opt. Express* **2014**, *22*, 6868–6873. [CrossRef]
19. Dong, Y.C.; Chertopalov, S.; Maleski, K.; Anasori, B.; Hu, L.; Bhattacharya, S.; Rao, A.M.; Gogotsi, Y.; Mochalin, V.N.; Podila, R. Saturable absorption in 2D Ti_3C_2 MXene thin films for passive photonic diodes. *Adv. Mater.* **2018**, *30*, 1705714. [CrossRef]
20. Wu, Q.; Jin, X.; Chen, S.; Jiang, X.; Hu, Y.; Jiang, Q.; Wu, L.; Li, J.; Zheng, Z.; Zhang, M.; et al. MXene-based saturable absorber for femtosecond mode-locked fiber lasers. *Opt. Express* **2019**, *27*, 10159–10170. [CrossRef]
21. Du, J.; Wang, Q.; Jiang, G.; Xu, C.; Zhao, C.; Xiang, Y.; Chen, Y.; Wen, S.; Zhang, H. Ytterbium-doped fiber laser passively mode locked by few-layer Molybdenum Disulfide (MoS_2) saturable absorber functioned with evanescent field interaction. *Sci. Rep.* **2014**, *4*, srep06346. [CrossRef] [PubMed]
22. Zhang, H.; Lu, S.B.; Zheng, J.; Du, J.; Wen, S.C.; Tang, D.Y.; Loh, K.P. Molybdenum disulfide (MoS_2) as a broadband saturable absorber for ultra-fast photonics. *Opt. Express* **2014**, *22*, 7249–7260. [CrossRef] [PubMed]
23. Xia, H.; Li, H.; Lan, C.; Li, C.; Zhang, X.; Zhang, S.; Liu, Y. Ultrafast erbium-doped fiber laser mode-locked by a CVD-grown molybdenum disulfide (MoS_2) saturable absorber. *Opt. Express* **2014**, *22*, 17341–17348. [CrossRef] [PubMed]
24. Woodward, R.I.; Howe, R.C.T.; Runcorn, T.H.; Hu, G.; Torrisi, F.; Kelleher, E.J.R.; Hasan, T. Wideband saturable absorption in few-layer molybdenum diselenide ($MoSe_2$) for Q-switching Yb-, Er-and Tm-doped fiber lasers. *Opt. Express* **2015**, *23*, 20051. [CrossRef]
25. Feldman, Y.; Wasserman, E.; Srolovitz, D.J.; Tenne, R. High-rate, gas-phase growth of MoS_2 nested inorganic fullerenes and nanotubes. *Science* **1995**, *267*, 222. [CrossRef]
26. Mao, D.; Du, B.; Yang, D.; Zhang, S.; Wang, Y.; Zhang, W.; She, X.; Cheng, H.; Zeng, H.; Zhao, J. Nonlinear Saturable Absorption of Liquid-Exfoliated Molybdenum/Tungsten Ditelluride Nanosheets. *Small* **2016**, *12*, 1489–1497. [CrossRef]
27. Woodward, R.I.; Kelleher, E.J.R. 2D Saturable Absorbers for Fibre Lasers. *Appl. Sci.* **2015**, *5*, 1440–1456. [CrossRef]
28. Yang, H.; Wang, Y.; Tiu, Z.C.; Tan, S.J.; Yuan, L.; Zhang, H. All-Optical Modulation Technology Based on 2D Layered Materials. *Micromachines* **2022**, *13*, 92. [CrossRef]
29. Luo, Z.; Wu, D.; Xu, B.; Xu, H.; Cai, Z.; Peng, J.; Weng, J.; Xu, S.; Zhu, C.; Wang, F.; et al. Two-dimensional material-based saturable absorbers: Towards compact visible-wavelength all-fiber pulsed lasers. *Nanoscale* **2016**, *8*, 1066–1072. [CrossRef]
30. Navarro-Moratalla, E.; Island, J.O.; Mañas-Valero, S.; Pinilla-Cienfuegos, E.; Castellanos-Gomez, A.; Quereda, J.; Rubio-Bollinger, G.; Chirolli, L.; Silva-Guillén, J.A.; Agraït, N.; et al. Enhanced superconductivity in atomically thin TaS2. *Nat. Commun.* **2016**, *7*, 11043. [CrossRef]
31. Zhao, Q.Y.; Guo, Y.H.; Zhou, Y.X.; Xu, X.; Ren, Z.; Bai, J.; Xu, X. Flexible and anisotropic properties of monolayer MX2 (M = Tc and Re; X = S, Se). *J. Phys. Chem. C* **2017**, *121*, 23744. [CrossRef]
32. Yin, J.; Zhu, F.; Lai, J.; Chen, H.; Zhang, M.; Zhang, J.; Wang, J.; He, T.; Zhang, B.; Yuan, J.; et al. Hafnium Sulfide Nanosheets for Ultrafast Photonic Device. *Adv. Opt. Mater.* **2019**, *7*, 1801303. [CrossRef]
33. Bachmann, R.; Kirsch, H.; Geballe, T. Optical properties and superconductivity of NbSe2. *Solid State Commun.* **1971**, *9*, 57–60. [CrossRef]
34. Huang, Y.H.; Chen, R.S.; Zhang, J.R. Electronic transport in $NbSe_2$two-dimensional nanostructures: Semiconducting characteristics and photoconductivity. *Nanoscale* **2015**, *7*, 18964–18970. [CrossRef] [PubMed]
35. Sohn, E.; Xi, X.; He, W.-Y.; Jiang, S.; Wang, Z.; Kang, K.; Park, J.-H.; Berger, H.; Forró, L.; Law, K.T.; et al. An unusual continuous paramagnetic-limited superconducting phase transition in 2D NbSe 2. *Nat. Mater.* **2018**, *17*, 504–508. [CrossRef]
36. Shi, Y.; Long, H.; Liu, S.; Tsang, Y.H.; Wen, Q. Ultrasmall 2D $NbSe_2$ based quantum dots used for low threshold ultrafast lasers. *J. Mater. Chem. C* **2018**, *6*, 12638–12642. [CrossRef]
37. Chen, L.; Du, L.; Li, J.; Yang, L.; Yi, Q.; Zhao, C. Dissipative Soliton Generation From Yb-Doped Fiber Laser Modulated by Mechanically Exfoliated NbSe2. *Front. Phys.* **2020**, *8*, 320. [CrossRef]
38. Yang, H. Niobium diselenide nanosheets for a vector soliton fiber laser. *J. Mater. Chem. C* **2020**, *8*, 14954–14958. [CrossRef]
39. Jin, L.; Zhang, Q.; Zhang, B.; Gao, Z.; Yang, S.; Li, L. Numerical analysis of hybrid mode-locking stability in a Ho-doped fiber laser. *Opt. Express* **2023**, *31*, 1141. [CrossRef]

Disclaimer/Publisher's Note: The statements, opinions and data contained in all publications are solely those of the individual author(s) and contributor(s) and not of MDPI and/or the editor(s). MDPI and/or the editor(s) disclaim responsibility for any injury to people or property resulting from any ideas, methods, instructions or products referred to in the content.